Complex-Valued Pipelined Recurrent Neural Network for Transmitter Distortions Compensation in High-Throughput Satellite Communication

Changzhi Xu[1,2(✉)], Yi Jin[2], Li Yang[2], Li Li[2], Mingyu Li[3], and Zhenxin Cao[1]

[1] State Key Laboratory of Millimeter Waves, Southeast University, Nanjing 210096, China
sandy_xu@126.com, 274630851@qq.com
[2] Xi'an Branch of China Academy of Space Technology, Xi'an 710000, China
john.0216@163.com, 87701726@qq.com, lili_504@126.com
[3] Chongqing University, Chongqing 400044, China
myli@cqu.edu.cn

Abstract. With the continuous development of satellite communication system towards the direction of high frequency band, large capacity and high spectral efficiency transmission, the signals processed by these new technologies have many characteristics, such as ultra-high bandwidth and higher peak-to-average power ratio (PAPR), etc., which puts forward a great challenge for the space-borne transmitter used in the satellite communication system. In view of the above requiremes, a novel digital predistortion (DPD) model based on complex-valued pipelined recurrent neural network (CPRNN) for joint compensation of wideband spaceborne transmitter is proposed in this paper. Once the CPRNN model is constructed, the complex-valued real time recurrent learning (CRTRL) algorithm is used for the CPRNN model training. Here, the CRTRL algorithm is derivated in detail based on the real-valued RTRL algorithm. The imperfect transmitters based on a GaN PA excited by the 400-MHz 64-amplitude/phase-shift keying (64APSK) signals was employed to verify the compensation performance of the proposed models. The simulation and experimental results show that the proposed CPRNN DPD model can achieve better linearization performance for the nonlinear transmitter with imperfect RF impairments.

Keywords: Digital predistortion (DPD) · Complex-valued pipelined recurrent neural network (CPRNN) · I/Q imbalance · Power amplifiers (PAs) · Satellite communication

1 Introduction

The inexorable pursuit of broadband satellite systems is motivating the transmission of broadband signals at symbol rates of multiple GHz(G) Baud rate. The high speed transmission demand of massive data promotes satellite communication to high frequency band, large bandwidth and high spectral efficiency. With the development of

Q. Wu et al. (Eds.): WiSATS 2020, LNICST 358, pp. 449–461, 2021.
https://doi.org/10.1007/978-3-030-69072-4_36

transmission direction, it is very important for nonlinear digital compensation of spaceborne RF transmitter. The MAPSK/MQAM and other multicarrier modulation, FDMA/TDMA/CDMA and other new technologies are widely used in the Gbps Baud code rate wireless transmission technology. Without exception, the signals processed by these new technologies are characterized by multi-carrier, multi-level, ultra-high bandwidth and peak to peak ratio, etc. For the RF transceiver front end, the new requirements caused by these characteristics must be considered, such as high efficiency and high linearity of the transmitter, etc. At the same time, the RF transceiver front end must be realized in a smaller volume. Because of the important role of RF transmitter in satellite communication and its serious influence on communication signals, the design and research of RF transmitter has always been an important subject in the development of satellite communication. On the one hand, the transmitter excited by wide bandwidth signals will present stronger and deeper nonlinear memory characteristics. Meanwhile, the RF transmitter system is inevitably affected by the nonlinear distortion of the amplifier, the modulator in-phase/quadrature (I/Q) imbalance, and the local oscillator (LO) leakage, etc. In addition, these different nonlinear characteristics will interact with each other, which seriously degrade the performance of the satellite communication system [1]. Therefore, it is the core technology to solve the reliable transmission of satellite communication in the future by researching a new type of broadband efficient linear transmitter, which make the RF front-end of wireless broadband transmission work efficiently under the premise of meeting the strict linearity of the system.

Compared with the RF and IF predistortion, baseband digital predistortion (DPD) does not involve RF signal processing and has become the most widely used predistortion scheme [2, 3]. Common baseband digital predistortion implementations include lookup tables [4, 5] and polynomials [6]. Recently, various methods have been proposed to compensate the interaction distortion between the PA nonlinearity and I/Q imbalance in transmitter [7–11]. For example, Ref. [8] analyzed the interaction between PA nonlinearity and IQ imbalance in detail, and studied the influence of I/Q orthogonal modem imbalance on adaptive digital predistortion parameter estimation. Some estimation methods have also been reported, where the effect of unbalanced coupling between PA and I/Q is considered in the compensation process. In addition, a novel rational function based conjugate model is proposed for alleviating the joint nonlinearity of the transmitter [7]. Furthermore, the dual-input nonlinear model based on the real value Volterra series is proposed in [11], this model can contain nonlinear frequency-related cross terms between the I and Q branch, where the nonlinear characteristics of radio frequency modulator can be modeled and compensated. However, the shortcoming in the dual-input compensator is that the nonlinear characteristics of the PA can not be considered. In order to solve the joint compensation problem of wideband transmitter, the method of joint estimation and compensation of frequency-dependent nonlinear distortions of the transmitter is proposed for the first time in literature [12]. This method can compensate all the analog front-end damages of the wideband direct frequency converter transmitter in one step estimation method, and the digital predistorter parameters can be extracteded without adding any additional RF hardware.

In recent years, with the rising and development of the artificial intelligence theory, people have applied the artificial intelligence theory to the wireless communication system, such as the establishment of PA behavioral model and the research of predistortion technology. In the past decade, artificial neural networks (ANNs) have been successfully applied in the fields of radio frequency and microwave circuit design domain [13, 14]. Artificial neural networks can be arbitrarily close to any continuous nonlinear function, and this method can be applied to transistor-level modeling [15] or more abstract system-level modeling [16, 17]. Recently, some modified NN models have been proposed for jointly compensating the transmitter distortions and impairments [17–19].

In this paper, a complex-valued pipelined recurrent neural network (CPRNN) model for nonlinear compensation of the transmitter distortions and impairments is proposed. To compare the different model performance, the RVFTDNN model [13], the parallel Hammerstein (PH) model [12], and the proposed CPRNN model were used to model and compensate the nonlinear characteristics of the transmitter. The simulation and exterimental results show that the the proposed CPRNN model can give the excellent performance for joint compensation of transmitter.

2 Proposed CPRNN Model Structure

It is the first step of constructing the transmitter behavioral model accurately for designing digital predistortion compensation system, so it is necessary to capture the main nonlinear characteristics of transmitter as a whole. In the transmitter, the mirror interference of IQ direct transform modulator will generate self-interference phenomenon, which causes the mirror interference generated by the transmitter to be located on the carrier frequency and in the same frequency band as the expected signal. Therefore, the transmitter behavioral model should capture all kinds of nonlinear sources as much as possible. When the NN theory is applied to transmitter behavioral modeling, it is necessary to study the regression method which is different from traditional fixed-model-based parameter identification. Mennwhile, the complex neural network structure and the complex training algorithm should be used in the transmitter behavioral modeling [20]. Usually, the inputs, the weights, and the outputs of the proposed NN structure are all complex-valued, and the training algorithm should also be extended to the complex domain.

The fully connected recurrent neural network (FCRNN) model structure is given in Fig. 1, which is consisted of L neurons and L feedback nodes. In order to increasing the approximation ability of the input signal, the orthogonal function extension defined as "FE" is proposed for representing the complex nonlinear dynamic systems. The input and the expansion using nonlinear polynomial can be given as

$$\begin{aligned} U(n) &= [u(n-1), u(n-2), \ldots, u(n-J)]^T \\ &= U^r(n) + jU^i(n) \end{aligned} \tag{1}$$

$$\begin{aligned} U_{FE}(n) &= FE(u(n-1), u(n-2), \ldots, u(n-J)) \\ &= [U_{FE,1}(n), U_{FE,2}(n), \ldots, U_{FE,J}(n)]^T \\ &= U_{FE}^r(n) + jU_{FE}^i(n) \end{aligned} \tag{2}$$

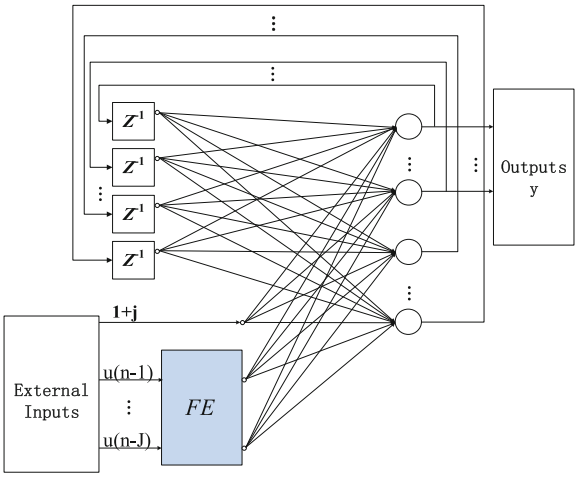

Fig. 1. FCRNN model sturcture

For the transmitter behavioral modeling, the I/Q components of the input signals and its nonlinear terms should be considered together [20]. Its corresponding input signal vector can be expressed as follows

$$\begin{aligned} U_{FE}(n) = [&1, u(n-1), u(n-2), \ldots, u(n-J), \\ &u(n-1)|u(n-2)|, \ldots, u(n-(J-1))|u(n-J)|, \\ &2u(n-1)|u(n-1)|-1, \ldots, 2u(n-J)|u(n-J)|-1, \\ &4u(n-1)|u^2(n-1)|-3u(n-1), \ldots, \\ &4u(n-J)|u^2(n-J)|-3u(n-J)]^T \end{aligned} \tag{3}$$

The entire network is constituted by a two-layer structure, where the external delay input layer and feedback output layer are the input for the model. In the proposed CPRNN model, the delayed input signals are extended by the "FE" nonlinear function, and the complex output of each neuron can be calcuted as $y_l(n)$. Then the entire input of the proposed network model can be expressed by the polynomial functional expansion of the input signals and feedback signals, which is given as follows

$$\begin{aligned} X(n) &= [S_{FE}(n), 1+j, y_1(n-1), y_2(n-1), \ldots, y_L(n-1)]^T \\ &= X_l^r(n) + jX_l^i(n), \quad l = 1, \ldots, p+L+1 \end{aligned} \tag{4}$$

Then, the *sth* neuron output in the CPRNN model can be defined as:

$$\begin{aligned} y_s(n) &= \varphi^r(u_s^r(n)) + j\varphi^i(u_s^i(n)) \\ &= y_s^r(n) + jy_s^i(n), s = 1, \ldots, L \end{aligned} \tag{5}$$

$$u_s(n) = \sum_{s=1}^{p+L-1} w_{l,s}(n) X_s(n) \tag{6}$$

Here, the complex-valued nonlinear activation function of the neuron is represented by φ, and the input signal of the activation function at time n can be represented by (6). Then the linear sum of all the output of the activation function after the weights are applied for the network output. The weight matrix of the CPRNN model is defined as

$$W = [\omega_1, \ \ldots, \omega_L] \tag{7}$$

where the weight vector in the network can be given as

$$\omega_l = [\omega_{l,1}, \ldots, \omega_{l,p+L+1}]^T \tag{8}$$

And the total length of the weight matrix is $(p + L + 1) * L$.

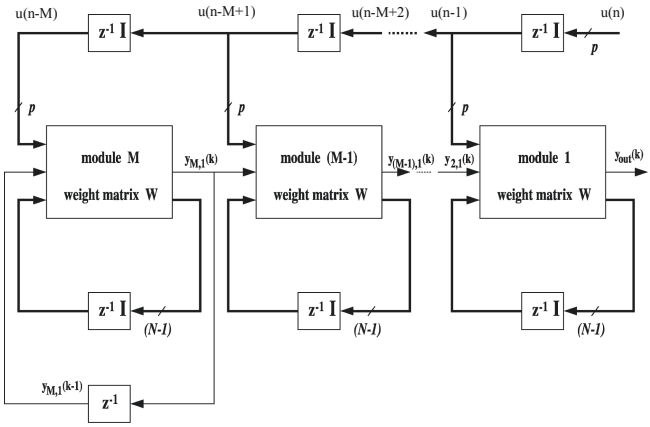

Fig. 2. CPRNN model structure for the transmitter

Furthermore, the complex-valued PRNN (CPRNN) can be designed using the proposed FCRNN structure, which is defined as an extension of real-valued PRNN and shown in Fig. 2. In the proposed CPRNN structure, the FCRNN with N neuron is the basic unit of each module. The $L - 1$ outputs of each module of the CPRNN are the feedback of the module input, the other outputs of each module are directly accessed to the next module. Then the complex-valued weight matrix of all modules in the CPRNN model can be given as

$$W(n) = [\omega_1(n), \ \ldots, \omega_l(n), \ \ldots, \omega_L(n)] \tag{9}$$

Accordingly, the complete expression of the CPRNN model is

$$\begin{aligned} y_{t,l}(n) \ &= \varphi^r(u_l^r(n)) + j\varphi^i(u_l^i(n)) \\ &= y_{t,l}^r(n) + jy_{t,l}^i(n), \quad t = 1, 2, \ \ldots, L \end{aligned} \tag{10}$$

here, $y_{t,l}(n)$ is the output of the *lth* neuron of the tth module at time n. For each module, the input vector can be defined as

$$X_t^T(n) = [U_{FE,t}(n), \ 1 + j, \ y_{t+1,1}(n-1), \ y_{t,2}(n-1), \ \ldots, \ y_{t,N}(n-1)] \tag{11}$$

$$X_M^T(n) = [U_{FE,M}(n),\ 1 + j, y_{M,1}(n-1), y_{M,2}(n-1),\ \ldots, y_{M,N}(n-1)] \tag{12}$$

where $X_t^T(n)$ is the input signal vector for the tth module, t = 1… M–1. $X_M^T(n)$ is input signal vector for the Mth module. As can be seen in Fig. 2, the input of the $M-1$ modules consists of the the output $y_{t+1,l}(n-1)$ of the last module, and the input of the last module M only contains the it's own feedback delay. Accordingly, the output of the first PRNN module is the total output of the network, which can be defined as

$$y_{out}(n) = y_{1,1}(n) \tag{13}$$

3 CRTRL Algorithm for CPRNN Model

According to the above model, the parameter extraction for the CPRNN model can be derived. Let $y_{t,1}(n)$ be the output of the module t, $d(n)$ is the real output signals of the transmitter, then the error signals of this module can be defined as

$$\varepsilon_t(n) = d(n-t+1) - y_{t,1}(n) = \varepsilon_t^r(n) + j\varepsilon_t^i(n) \tag{14}$$

$$\begin{aligned} \varepsilon_t^r(n) &= d^r(n-t+1) - y_{t,1}^r(n) \\ \varepsilon_t^i(n) &= d^i(n-t+1) - y_{t,1}^i(n) \end{aligned} \tag{15}$$

Then the complex cost function can be defined as [21]

$$\begin{aligned} J(n) &= \sum_{t=1}^{M} \lambda^{t-1}(n)|\varepsilon_t(n)|^2 \\ &= \sum_{t=1}^{M} \lambda^{t-1}(n)[\varepsilon_t(n)\varepsilon_t^*(n)] \\ &= \sum_{t=1}^{M} \lambda^{t-1}(n)[(\varepsilon_t^r)^2 + (\varepsilon_t^i)^2] \end{aligned} \tag{16}$$

Where $\lambda(n)(0 < \lambda \leq 1)$ is the forgetting factor. The weight can be updated in the steepest descent direction

$$\Delta\omega_{l,s}(n) = -\eta \frac{\partial}{\partial\omega_{l,s}(n)} \left(\sum_{t=1}^{M} \lambda^{t-1}(n)|\varepsilon_t(n)|^2 \right) \tag{17}$$

Then the sensitive function for each module of the CPRNN model at the time n can be defined as [22]

$$\begin{bmatrix} \Lambda_{l,s,t}^{rr,j}(n) & \Lambda_{l,s,t}^{ri,j}(n) \\ \Lambda_{l,s,t}^{ir,j}(n) & \Lambda_{l,s,t}^{ii,j}(n) \end{bmatrix} = \begin{bmatrix} \dfrac{\partial y_{t,j}^r(n)}{\partial\omega_{l,s}^r(n)} & \dfrac{\partial y_{t,j}^r(n)}{\partial\omega_{l,s}^i(n)} \\ \dfrac{\partial y_{t,j}^i(n)}{\partial\omega_{l,s}^r(n)} & \dfrac{\partial y_{t,j}^i(n)}{\partial\omega_{l,s}^i(n)} \end{bmatrix} \tag{18}$$

According to the definition of the sensitive function matrix, the changing degree of the *lth* neuron output to the weight can be represented by the element. And the update equation for the sensitive functions can be given as

$$\begin{aligned}\begin{bmatrix}\Lambda_{l.s,t}^{rr}(n) & \Lambda_{l.s,t}^{ri}(n)\\ \Lambda_{l.s}^{ir}(n) & \Lambda_{l.s}^{ii}(n)\end{bmatrix} &= \begin{bmatrix}\varphi\psi^{r}(n-1) & 0\\ 0 & \varphi\psi^{i}(n-1)\end{bmatrix}\\ \times\left\{\sum_{\alpha=1}^{N}\left(\begin{bmatrix}\omega_{l,\alpha+p+1}^{r}(n-1) & -\omega_{l,\alpha+p+1}^{i}(n-1)\\ \omega_{l,\alpha+p+1}^{r}(n-1) & \omega_{l,\alpha+p+1}^{i}(n-1)\end{bmatrix}\right.\right.&\\ \left.\left.\times\begin{bmatrix}\Lambda_{l.s,t}^{rr,\alpha}(n-1) & \Lambda_{l.s,t}^{ri,\alpha}(n-1)\\ \Lambda_{l.s,t}^{ir,\alpha}(n-1) & \Lambda_{l.s,t}^{ii,\alpha}(n-1)\end{bmatrix}\right)&\\ +\begin{bmatrix}\delta_{\ln}X_{s}^{r}(n-1) & -\delta_{\ln}X_{s}^{i}(n-1)\\ \delta_{\ln}X_{s}^{i}(n-1) & \delta_{\ln}X_{s}^{r}(n-1)\end{bmatrix}\right\}&\end{aligned} \tag{19}$$

Further simplify:

$$\begin{aligned}(\Lambda_{l,n}^{t}(n))^{*} &= \left\{\psi^{*}(n)\right\}'\\ \times\left[\sum_{\alpha=1}^{N}\omega_{l,\alpha+p+1}^{*}(n)\left(\Lambda_{l,s}^{t,\alpha}(n-1)\right)^{*}+\delta_{\ln}X_{t,s}^{*}(n)\right]&\end{aligned} \tag{20}$$

Finally, the update equation for the weight of the CPRNN model can be obtained

$$\begin{aligned}\omega_{l,s}(n+1) &= \omega_{l,s}(n)\\ +\eta\left(\sum_{t=1}^{M}\lambda^{t-1}(n)e_{t}(n)\{\varphi^{*}(u_{t,l}(n))\}'\right.&\\ \left.\times\left[\sum_{\alpha=1}^{N}\omega_{1,\alpha+p+1}^{*}(n)\left(\Lambda_{l,s}^{t,\alpha}(n-1)\right)^{*}+\delta_{\ln}X_{t,s}^{*}(n)\right]\right)&\end{aligned} \tag{21}$$

4 Simulation and Experimental Results

In order to verify the performance of the proposed CPRNN model, the behavioral model for the transmitter is carried out firstly. Here, the normalized mean square error (NMSE) is adopted to evaluate the model accuracy [20]. The RVFTDNN model [13], the parallel Hammerstein (PH) model [12], and the FCRNN model are selected for the transmitter model performance comparison. In this section, a wideband high-efficiency GaN Class-AB PA over 27–31 GHz is designed for the experimental verification. The Class-F PA worked at 29 GHz, which has the average output power of 36 dBm. The baseband input signals are the high-order spectrally-efficient 64 amplitude/phase-shift keying (64APSK) modulations, which are adopted widely in Satellite communication system [23]. The synthesized 64APSK signals have a signal bandwidth of 400 MHz and are sampled at 3.2 GHz. Considering the practical application, the I/Q imbalance, dc-offset and

PA nonlinear distortions of the transmitter are all considered together. The amplitude imbalance of the I/Q branch is set to 2 dB, and the phase imbalance of the I/Q branch is set to 3°. And the dc-offset values for the I and Q channel are set to 3% and 5%, respectively.

The structure of the FCRNN model, the CPRNN model and the RVFTDNN model can be detemined using the trial and error method. Finally, the number of input and output neurons of the FCRNN model is set to 4, the forgetting factor $\lambda = 0.5$, and the learning rate $\eta = 0.05$. The structure and parameter settings for each module in the CPRNN model are set to the same, which is consists of M FCRNN modules. Here the the value of M is set to 4 by using the trial and error method. The structure of the RVFTDNN model is a three-layer network, and the numbers of neurons in the hidden layers can be determined by the optimization process, which is 7 and 15, respectively, and output layer contains two linear neurons. Once the structure of these models is determined, the corresponding comparison results of these compensation models are obtained in Table 1 in detail. As can be seen in the table, the CPRNN model has more accurate modeling effect for the transmitter, which can give 4 dB improvement of NMSE value than the conventional PH model.

Table 1. Model performance comparison

Model	Neurons	NMSE(dB)
PH model	P = 9, M = 3	−34.87
RVFTDNN	7-15-2	−36.83
FCRNN	P = 4, N = 4	−36.55
CPRNN	P = 4, N = 4, M = 4	−38.76

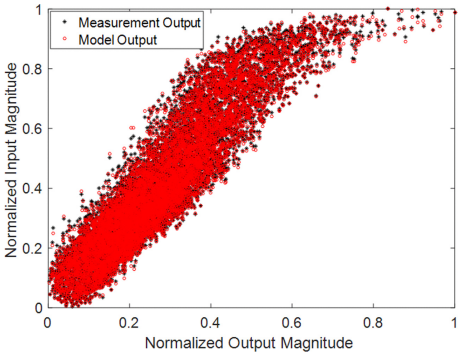

Fig. 3. The dynamic AM/AM characteristics comparison from the measurement output and the model predicted output

Considering the nonlinear memory effects of the transmitter, the amplitude and phase of the transmitter output signals will change nonlinearly with the amplitude of the input

signal, and the I/Q imbalance and dc-offset will further exacerbate its distortion. To represent the nonlinear characteristics of the transmitter, the the dynamic AM/AM and AM/PM curves of the measured output and the modeled output are given in Fig. 3 and Fig. 4, respectively. As can be seen from the figures, the proposed CPRNN model can replicate the nonlinear curve well. It can be concluded that the CPRNN model can describes the nonlinear imfluence of the transmitter I/Q imbalance and dc offset on the gain and phase distortions.

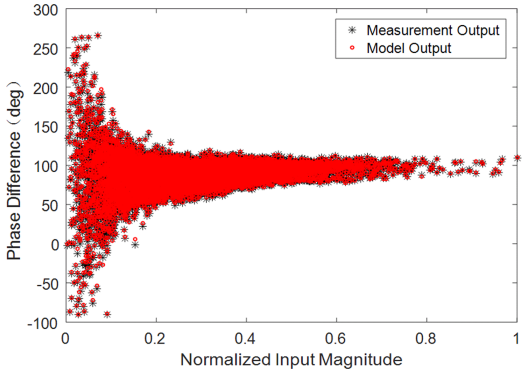

Fig. 4. The dynamic AM/PM characteristics comparison from the measurement output and the model predicted output

Furthermore, the power spectrum density (PSD) of the 64APSK signals can be plotted for the comparison of the model performance in the frequency domain. Figure 5 presents the PSD comparison of the model prediction outputs and the experimental outputs. The lower the frequency spectrum of the error signal, the better the prediction performance of the model.

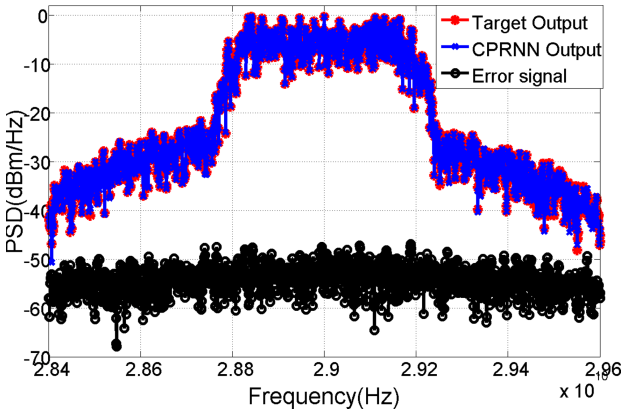

Fig. 5. Measured and modeled PSD comparison of 64APSK signals

The accurate model performance of the CPRNN model has been validated in the previous section. In theory, the more accurate the behavior model results, the better the linearization results. In order to verify the performance of the CPRNN model in the DPD system, the proposed model is applied to a complete transmitter system, where the PA nonlinearities, I/Q imbalance and dc-offset are considered together. According to the obtained input and output signals of the transmitter, the DPD inverse model can be obtained. Then the transmitter input signals can be processed through the inverse model to get the DPD signals. Then, the DPD output signals pass through the transmitter to get the linearizaed results of the transmitter.

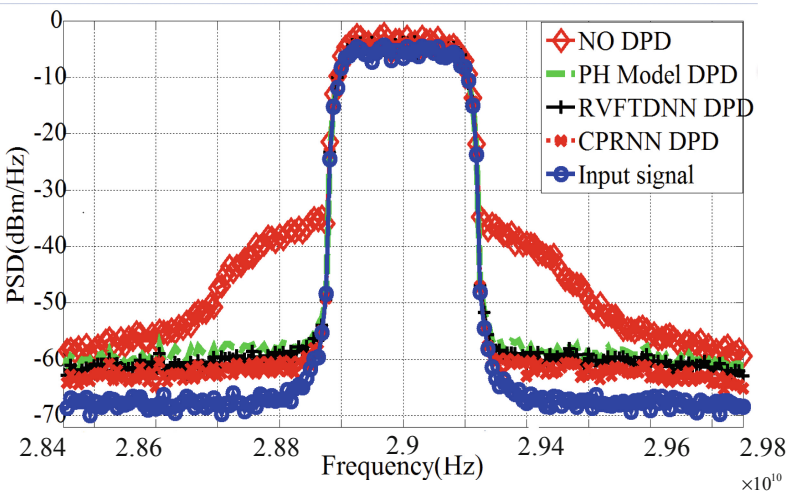

Fig. 6. DPD comparison of different models for 64APSK signal

Table 2. ACPR performance of different models.

DPD Models	ACPR(dB)	
	−200MHz	+200 MHz
Without DPD	−36.49	−37.76
PH DPD	−51.85	−52.02
RVFTDNN	−53.63	−53.46
CPRNN	−55.44	−55.26
Input Signals	−59.88	−59.89

In order to obtain the linearized results of the different predistorters the proposed 64APSK modulation signals are used for practical experimental validation in the transmitter system. The first is the comparison of the PSD after linearization, which

is given in Fig. 6. It can be seen from the figure that the PSD of the transmitter distortion outputs can be compensated to different degrees by these DPD models. Here, the PH DPD models presents the worst compensation effect. The compensation results of the RVFTDNN and the FCRNN DPD model almost have the same linearization results, and the linearized results of the proposed CPRNN model presents the best ACPR results. The quantitative representation of the linearization results is given in Table 2. As can be seen from Table 2, only 15 dB ACPR improvement can be obtained by the PH DPD model. And the RVFTDNN and the FCRNN DPD model can give the ACPR improvement of about 17 dB. As a comparison, the proposed CPRNN DPD model can achieve 19 dB ACPR improvement. Both the measured and quantitative results prove that the proposed CPRNN DPD model can compensate jointly the nonlinear distortions and RF impairments of the transmitter very well.

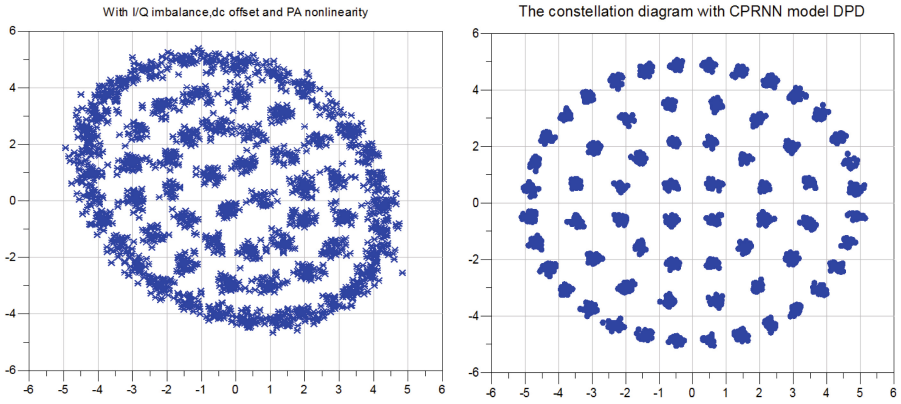

Fig. 7. Constellation diagrams of 64APSK signals. (a) shows the constellation diagram without DPD. (b) shows the constellation diagram with CPRNN model DPD.

The constellation diagrams of 64APSK modulation is given in Fig. 7, where Fig. 7(a) shows the constellation diagram without DPD and Fig. 7(b) shows the constellation diagram with CPRNN DPD model. As can be seen in Fig. 7, the distortions of the 64APSK constellation in Fig. 7(a) can be significantly compensated using the proposed CPRNN DPD model, and the compensated constellation diagrams in Fig. 7(b) can be used directly for digital demodulation.

5 Conclusion

In this paper, the CPRNN model consisted of the M-order FCRNN module is proposed for transmitter joint compensation. For the model parameter extraction, and the CRTRL learning algorithm is derived in detaill. The orthogonal polynomial structure is used in the PRNN structure for fitting the nonlinear characteristics of the transmitter. In practice, the

optimal model order M and the appropriate complex activation function of the CPRNN model can be obtained through the iterative simulations. To verify the linearization ability of the proposed model, the GaN Class-AB PA driven by the 400MHz 64APSK signals including quadrature modulator I/Q imbalance and dc offset is used for the experimental measurements. Experimental results show that the proposed CPRNN DPD model can give better linearization results for the transmitter including I/Q imbalance and dc-offset compared with the other common compensation models when the complex-valued signals of the transmitter is processed simultaneously.

References

1. Harris, F.: Digital filter equalization of analog gain and phase mismatch in I-Q receivers. In: Proceedings of ICUPC - 5th International Conference on Universal Personal Communications, Cambridge, MA, USA, vol. 2, pp. 793–796 (1996)
2. Ding, L., Zhou, G.T.: Effects of even-order nonlinear terms on power amplifier modeling and predistortion linearization. IEEE Trans. Veh. Technol. **53**(1), 156–162 (2004)
3. Yu, X., Jiang, H.: Digital predistortion using adaptive basis functions. IEEE Trans. Circ. Syst. I Regul. Pap. **60**(12), 3317–3327 (2013)
4. Muhonen, K.J., Kavehrad, M., Krishnamoorthy, R.: Look-up table techniques for adaptive digital predistortion: a development and comparison. IEEE Trans. Veh. Technol. **49**(5), 1995–2002 (2000)
5. Cavers, J.K.: Amplifier linearization using a digital predistorter with fast adaptation and low memory requirements. IEEE Trans. Veh. Tech. **39**(4), 374–382 (1990)
6. Braithwaite, R.N.: Digital predistortion of an RF power amplifier using a reduced Volterra series model with a memory polynomial estimator. IEEE Trans. Microw. Theory Tech. **65**(10), 3613–3623 (2017)
7. Aziz, M., Rawat, M., Ghannouchi, F.: Rational function based model for the joint mitigation of I/Q imbalance and PA nonlinearity. IEEE Microw. Wirel. Comp. Lett. **23**(4), 196–198 (2013)
8. Cavers, J.: The effect of quadrature modulator and demodulator errors on adaptive digital predistorters for amplifier linearization. IEEE Trans. Veh. Technol. **46**(2), 456–466 (1997)
9. Kim, Y., Jeong, E., Lee, Y.: Adaptive compensation for power amplifier nonlinearity in the presence of quadrature modulation/demodulation errors. IEEE Trans. Sig. Process. **55**(9), 4717–4721 (2007)
10. Hilborn, D., Stapleton, S., Cavers, J.: An adaptive direct conversion transmitter. IEEE Trans. Veh. Technol. **43**(2), 223–233 (1994)
11. Cao, H., Tehrani, A., Fager, C., Ericsson, T., Zirath, H.: I/Q imbalance compensation using a nonlinear modeling approach. IEEE Trans. Microw. Theory Techn. **57**(3), 513–518 (2009)
12. Anttila, L., Handel, P., Valkama, M.: Joint Mitigation of power amplifier and I/Q modulator impairments in broadband direct-conversion transmitters. IEEE Trans. Microw. Theory Tech. **58**(4), 730–739 (2010)
13. Rawat, M., Rawat, K., Ghannouchi, F.M.: Adaptive digital predistortion of wireless power amplifiers/transmitters using dynamic real-valued focused time-delay line neural networks. IEEE Trans. Microw. Theory Tech. **58**(1), 95–104 (2010)
14. Liu, T., Boumaiza, S., Ghannouchi, F.M.: Dynamic behavioral modeling of 3G power amplifiers using real-valued time-delay neural networks. IEEE Trans. Microw. Theory Tech. **52**(3), 1025–1033 (2004)

15. Woo, Y.Y., et al.: Feedforward amplifier for WCDMA base stations with a new adaptive control method. In: IEEE MTT-S International Microwave Symposium Digest, vol. 2, pp. 769–772 (2002)
16. Isaksson, M., Wisell, D., Ronnow, D.: Wide-band dynamic modeling of power amplifiers using radial-basis function neural networks. IEEE Trans. Microw. Theory Tech. **53**(11), 3422–3428 (2005)
17. Wang, D., Aziz, M., Helaoui, M., Ghannouchi, F.M.: Augmented real-valued time-delay neural network for compensation of distortions and impairments in wireless transmitters. IEEE Trans. Neural Netw. Learn. Syst. **30**(1), 242–254 (2019)
18. Jaraut, P., Rawat, M., Ghannouchi, F.M.: Composite neural network digital predistortion model for joint mitigation of crosstalk, I/Q imbalance, nonlinearity in MIMO transmitters. IEEE Trans. Microw. Theory Tech. **66**(11), 5011–5020 (2018)
19. Lajnef, S., Boulejfen, N., Abdelhafiz, A., Ghannouchi, F.M.: Two-dimensional cartesian memory polynomial model for nonlinearity and I/Q imperfection compensation in concurrent dual-band transmitters. IEEE Trans. Circ. Syst. II Exp. Briefs **63**(1), 14–18 (2016)
20. Li, M., Liu, J., Jiang, Y., Feng, W.: Complex-Chebyshev functional link neural network behavioral model for broadband wireless power amplifiers. IEEE Trans. Microw. Theory Tech. **60**(6), 1979–1989 (2012)
21. Haykin, S., Li, L.: Nonlinear adaptive prediction of nonstationary signals. IEEE Trans. Sig. Process. **43**(2), 526–535 (1995)
22. Kechriotis, G., Manolakos, E.S.: Training fully recurrent neural networks with complex weights. IEEE Trans. Circ. Syst. II Analog Digit. Sig. Process. **41**(3), 235–238 (1994)
23. Morello, A., Mignone, V.: DVB-S2: the second generation standard for satellite broad-band services. Proc. IEEE **94**(1), 210–227 (2006)